Local Suppression of Pro-Inflammatory Cytokines and the Effects in BMP-2-Induced Bone Regeneration

Juthamas Ratanavaraporn, Hiroyuki Furuya, and Yasuhiko Tabata*

Institute for Frontier Medical Sciences, Kyoto University, 53 Kawara-cho Shogoin, Sakyo-ku, Kyoto 606-8507, Japan

** Corresponding author. Tel.: +81 75 751 4128; fax: +81 75 751 4646*

E-mail address: yasuhiko@frontier.kyoto-u.ac.jp (Y. Tabata)

Abstract

The objective of this study is to investigate the effect of local inflammation suppression on the bone regeneration. Gelatin hydrogels incorporating mixed immunosuppressive triptolide-micelles and bone morphogenic protein-2 (BMP-2) were prepared. The controlled release of both the triptolide and BMP-2 from the hydrogels was observed under *in vitro* and *in vivo* conditions. When either J774.1 macrophage-like or MC3T3-E1 osteoblastic cells were cultured in the hydrogels incorporating mixed 2.5, 5 or 10 mg of triptolide-micelles and BMP-2, the expression level of pro- and anti-inflammatory cytokines including interleukin (IL)-6 and IL-10 was down-regulated, but the alkaline phosphatase (ALP) activity was promoted compared with those of hydrogels incorporating BMP-2 without triptolide-micelles. When implanted into a critical-sized bone defect of rats, the hydrogels incorporating mixed 2.5 or 5 mg of triptolide-micelles and BMP-2 showed significantly lower number of neutrophils, lymphocytes, macrophages or dendritic and mast cells infiltrated into the defect, and lower expression level of IL-6, TNF-α, and IL-10 than those incorporating BMP-2 without triptolide-micelles. The reduced local inflammation responses at the defects implanted with the hydrogels incorporating mixed 2.5 or 5 mg of triptolide-micelles and BMP-2 subsequently enhanced the bone regeneration thereat. It is concluded that the proper local modulation of inflammation responses is a promising way to achieve the enhanced bone regeneration.

Key words: Inflammation suppression, pro-inflammatory cytokines, bone regeneration, triptolide, bone morphogenic protein-2 (BMP-2), controlled release

1. Introduction

Bone regeneration involves complex physiological processes which are initiated with the local inflammation responses, followed by the mobilization of hematopoietic (HSC) and mesenchymal stem cells (MSC) to the site to form vascular networks, soft matrix tissues, cartilage, and bone. The process consists of a well-orchestrated time sequence of events to regulate the proliferation of stem cells and their differentiation into vascular-forming endothelial cells and bone-forming osteoblasts [1,2]. As it is recognized that the local inflammation step is required to initiate the subsequent process of tissue regeneration, the proper responses of inflammation are substantially necessary to guide the normal regeneration of damaged tissues [3]. On the other hand, deficient or excessive inflammation would biologically modify some subsequent signaling molecules, and consequently inhibit or delay the tissue regeneration [4-6]. It is demonstrated that some inflammatory molecules, e.g. pro-inflammatory cytokines including interleukin (IL)-1, IL-6, and tumor necrosis factor (TNF)-α, can induce the release of secondary signaling molecules and to recruit cells necessary for tissue regeneration [7]. Absence of the pro-inflammatory cytokines often impairs the process of tissue healing [8]. Over-expression of pro-inflammatory cytokines causes the catabolic effects on the quantity and quality of tissue regeneration [9-11]. Therefore, it is highly conceivable that a fine balance in the cellular interaction and cytokine expression between the inflammation and regeneration processes is practically a key to modify the final result of damaged tissue regeneration.

In recent, the modulation of inflammation with some drugs aiming at the enhancement of tissue regeneration has been increasingly investigated [5,7,12,13]. Among the drug candidates, triptolide, a natural product isolated from the Chinese herb *Tripterygium wilfordii Hook F.*, is one of potent compounds for immunosuppression and anti-inflammation treatments

[14-20]. Triptolide is a well-tolerated small molecule which has been widely used to treat inflammation and autoimmune diseases, such as rheumatoid arthritis of a traditional Chinese medicine [21]. Many researches have attempted to explore the suppression mechanism of triptolide-mediated inflammation both *in vitro* and *in vivo*. It is reported that triptolide has an inhibitory effect on the activation of T cells and their gene transcription of pro-inflammatory cytokines [14,15]. In addition, it can induce apoptosis in T and dendritic cells by inhibiting a nuclear factor kappa-light-chain-enhancer of activated B cells (NF-κB) transcription [16,17]. Wei *et al.* reported that the administration of triptolide intraperitoneally every other days for 8 weeks significantly reduced the numbers of CD4-positive T cells and macrophages in lamina propria and decreased the production of TNF-α and interferon (IFN)-γ in the colon of IL-10 deficient mice [22]. Triptolide can suppress the differentiation of immature human monocytes as well as reduce a capacity of monocytes to stimulate the proliferation of lymphocyte in the allogeneic mixed lymphocyte reaction [23]. It also inhibited the migration of dendritic cells into tissues by inhibiting the expression of chemokine (C-C motif) receptor (CCR)-7 and cyclooxygenase (COX)-2 through phosphoinositide 3-kinase (PI3-K)/Akt and NF-κB pathways [24]. In addition, some clinical and experimental studies have demonstrated that the administration of triptolide by the oral route effectively prolonged the allograft survival in the transplantation of some organs including bone marrow, cardiac, renal, and skin tissues [18,19,24]. However, up to date, triptolide does not always have a wide therapeutic window because of its water-insolubility and dose-dependent toxicity. The effective dose of tirptolide is nearly equal to the toxic dose that shows adverse side effects of reversible skin irritation and other systemic responses [20]. To overcome the drawbacks, a controlled delivery of triptolide specifically to the desired site in the body should be designed to decrease or avoid the side effect at the non-target sites. The local delivery system can also reduce the dose required, prevent the first-pass metabolism, and provide the rapid action of drug at the target site.

The objective of this study is to investigate bone morphogenic protein-2 (BMP-2)-induced bone regeneration under a condition of inflammation suppression. Bone regeneration at a critical-sized defect or a subcutaneous site is achieved by the controlled release of BMP-2 from gelatin hydrogels [25-27]. The triptolide of water-insoluble property was encapsulated into the micelles of a hydrophobic gelatin derivative to allow it to solubilize in water. The water-soluble triptolide-micelles were incorporated into the gelatin hydrogels to achieve the controlled release. The local suppression of inflammation induced by the triptolide release was evaluated in terms of the number of inflammatory cells infiltrated and the level of pro-inflammatory cytokines.

In this study, gelatin hydrogels incorporating mixed various doses of triptolide-micelles and BMP-2 were fabricated. The *in vitro* and *in vivo* profiles of triptolide and BMP-2 release from gelatin hydrogels and the hydrogels degradation were investigated. The *in vitro* culture of macrophage-like and pre-osteoblastic cells in the hydrogels incorporating BMP-2 with or without the triptolide-micelles was carried out to compare the expression level of pro-inflammatory cytokines and the osteogenic differentiation. After the hydrogels implantation into a critical-sized bone defect model of rats, the inflammation responses and bone regeneration were qualitatively and quantitatively evaluated in terms of histological and immunohistrochemical, real-time polymerase chain reaction (PCR), radiology, micro-computed tomography (μCT), and peripheral quantitative computed tomography (pQCT) examinations.

2. Materials and methods

2.1. Materials

A gelatin sample prepared by an acidic treatment of porcine skin collagen (isoelectric point (IEP) = 9.0) was kindly supplied by Nitta Gelatin Inc., Osaka, Japan. Recombinant human bone morphogenetic protein-2 (BMP-2) was kindly supplied from Yamanouchi Pharmaceutical Co., Tokyo, Japan. Triptolide (IUPAC name: (3bS,4aS,5aS,6R,6aR,7aS,7bS, 8aS,8bS)-3b,4,4a,6,6a,7a,7b,8b,9,10-decahydro-6-hydroxy-6a-isopropyl-8b-methyltrisoxireno [6,7:8a,9:4b,5] phenanthro [1,2-c] furan-1 (3H)-one, the molecular weight = 360.4) was purchased from Tocris Bioscience Inc., Ellisville, MO. $Na^{125}I$ (NEZ-033H, >12.95 GBq/ml) and N'-succinimidyl-3-(4-hydroxy-3,5-di[125I]iodophenyl)propionate or [^{125}I] Bolton-Hunter reagent (NEX-120H, 147 MBq/ml) were purchased from Perkine Elmer Life Sciences Inc., Boston, MA. Disuccinimidyl carbonate (DSC) and 4-dimethylaminopyridine (DMAP) were obtained from Nacalai Tesque Inc., Kyoto, Japan. Glutaraldehyde, glycine, dimethyl sulfoxide (DMSO), and other chemicals were obtained from Wako Pure Chemical Industries, Ltd., Osaka, Japan and used without further purification. All the primers (Table 1) were purchased from Invitrogen Corporation, Ltd., Carlsbad, CA.

2.2. Synthesis of L-lactic acid oligomer-grafted gelatin

L-lactic acid oligomer with the number-average molecular weight of 1,000 was synthesized from L-lactide monomer by the ring-opening polymerization, as published previously [33]. L-lactic acid oligomer (3×10^{-5} mole) was dissolved in 15 ml DMSO, while DSC (9×10^{-5} mole) and DMAP (9×10^{-5} mole) were dissolved in 2.5 ml of DMSO. The solution was mixed to allow the reaction for 3 hr under stirring at room temperature to activate the hydroxyl groups of L-lactic acid oligomer. The solution of activated L-lactic acid oligomer

was slowly added to the gelatin (IEP = 5) solution in DMSO (33 mg/ml), and the mixture was stirred overnight at room temperature to chemically graft the L-lactic acid oligomer to gelatin. The resulting solution was dialyzed against double-distilled water (DDW) using a dialysis tube (molecular weight cut off = 12,000–14,000) at room temperature for 72 hr, followed by freeze-drying to obtain the L-lactic acid oligomer-grafted gelatin. The ratio of L-lactic acid oligomer grafted to the amino groups of gelatin determined by fluorescamine assay was 3.1 ± 0.8 mole/mole gelatin, as reported previously [33].

2.3. Preparation of L-lactic acid oligomer-grafted gelatin and triptolide micelles

L-lactic acid oligomer-grafted gelatin solution (1 mg/ml) in DMSO and triptolide solution (1 mg/ml) in DMSO were prepared. The triptolide solution (1 ml) was added to the L-lactic acid oligomer-grafted gelatin solution (30 ml), followed by stirring at room temperature for 3 hr. The reaction mixture was dialyzed using a dialysis tube (molecular weight cut off = 1,000) for 72 hr. The dialysate obtained was centrifuged at 8,000 rpm, 4 °C for 10 min to separate water-insoluble triptolide, and freeze-dried to obtain the triptolide water-solubilized by L-lactic acid oligomer-grafted gelatin micelles (triptolide-micelles). To measure the amount of triptolide incorporated into the micelles, the triptolide-micelles freeze-dried were dissolved in 100 vol% ethanol. The solution absorbance was measured at a wavelength of 210 nm while the triptolide concentration was determined from the calibration curve prepared with the 100 vol% ethanol containing various amounts of triptolide.

2.4. Preparation of gelatin hydrogels incorporating triptolide-micelles and BMP-2

Hydrogels were prepared through the chemical crosslinking of gelatin with glutaraldehyde according to the method described previously [25,33]. Briefly, a solution (100 μl) containing 0, 2.5, 5 or 10 mg of triptolide-micelles was added to 400 μl of gelatin (IEP =

9.0) solution (50 mg/ml). Then, the solution was mixed with glutaraldehyde solution at a concentration of 0.16 vol%, and cast into a Tissue-Tek® mold (10 mm×10 mm, Sakura Finetek Japan Co., Ltd., Tokyo, Japan), followed by leaving at 4 °C for 12 hr for gelatin crosslinking. The hydrogels were agitated in 100 mM aqueous glycine solution at room temperature for 2 hr to block the residual aldehyde groups of glutaraldehyde. Following washing three times with DDW, the hydrogels were freeze-dried and sterilized by ethylene oxide. Prior to the following experiments, BMP-2 (5 μg) solution was adsorbed onto each hydrogel freeze-dried (1 x 2 x 6 mm^3), followed by leaving at 4 °C overnight for the solution incorporation to obtain gelatin hydrogels incorporating mixed triptolide-micelles and BMP-2.

2.5. In vitro and in vivo release studies of triptolide from gelatin hydrogels

For the *in vitro* release study of triptolide, gelatin hydrogels incorporating 0, 2.5, 5 or 10 mg of triptolide-micelles and 5 μg of BMP-2 were incubated in 1 ml of 100 mM phosphate-buffered saline solution (PBS, pH 7.4) at 37 °C. At each time point, the PBS supernatant was collected and replaced with fresh PBS. The PBS supernatant containing triptolide released was freeze-dried, and then the sample was re-dissolved in 100 vol% ethanol. The triptolide amount was determined by measuring the solution absorbance similarly. The experiment was independently performed for 4 samples per experimental group at each sampling point.

For the *in vivo* release study of triptolide, the hydrogels incorporating 0, 2.5, 5 or 10 mg of triptolide-micelles and 5 μg of BMP-2 were implanted into the back subcutis of 6-week-old female ddY mice (18–20 g body weight, Shimizu Laboratory Supply, Kyoto, Japan). At different time intervals, the hydrogel was collected and incubated with 1 ml collagenase solution (1 mg/ml) at 37 °C until to the complete digestion. The resulting solution was freeze-dried, and then the sample was re-dissolved in 100 vol% ethanol, followed by the similar

determination of triptolide amount. The experiment was independently performed for 3 samples per experimental group at each sampling point.

2.6. In vitro and in vivo release studies of BMP-2 from gelatin hydrogels

BMP-2 was radioiodinated according to the conventional chloramine T method as previously described [34]. Briefly, 5 μl of $Na^{125}I$ was added into 200 μl of BMP-2 solution (150 μg/ml) in 0.5 M potassium phosphate-buffered solution (pH 7.5) containing 0.5 M NaCl. Then, 100 μl of the same buffer containing 0.2 mg/ml chloramine-T was added to the solution mixture. After vortex mixing at room temperature for 2 min, 100 μl of PBS containing 0.4 mg sodium metabisulfate was added to the reacting solution to stop the radioiodination. The solution mixture was passed through a PD-10 desalting column (GE Healthcare Life Sciences, Chalfont St Giles, UK) to remove the uncoupled, free ^{125}I molecules from the ^{125}I-labeled BMP-2 using PBS as an eluting solution. PBS solution containing ^{125}I-labeled BMP-2 (14 μg/ml) was mixed with PBS containing non-labeled BMP-2 to give the final concentration of 500 μg/ml. The mixed solution containing 5 μg of BMP-2 (10 μl) was then adsorbed onto the hydrogel incorporating triptolide-micelles freeze-dried (1 x 2 x 6 mm^3), followed by leaving at 4 °C overnight to allow the solution to impregnate into the hydrogel. The gelatin hydrogels incorporating mixed 0, 2.5, 5 or 10 mg of triptolide-micelles and 5 μg of ^{125}I-labeled BMP-2 were obtained.

For the *in vitro* release study, the hydrogel incorporating mixed various doses of triptolide-micelles and BMP-2 was incubated in 1 ml of PBS solution (pH 7.4) at 37 °C. At each time-point, the PBS supernatant was collected and replaced with fresh PBS. The radioactivity of PBS supernatant was measured by the gamma counter (Auto Well Gamma System ARC-380 CL, Aloka Co., Ltd, Tokyo, Japan). The experiment was independently performed for 4 samples per experimental group at each sampling point.

For the *in vivo* release study, the hydrogel was implanted into the back subcutis of 6-week-old female ddY mouse. At different time intervals, the hydrogels were taken out to measure the radioactivity remaining by the gamma counter. The experiment was independently performed for 3 samples per experimental group at each sampling point.

2.7. In vivo degradation studies of gelatin hydrogels

To evaluate the *in vivo* degradation profiles of hydrogels, the implantation of ^{125}I-labeled hydrogels was performed according to the method previously reported [35]. Briefly, 20 μl of [^{125}I]Bolton–Hunter reagent solution in benzene was completely evaporated at room temperature. The resultant solid reagent was re-dissolved in 1 ml of PBS and the resulting solution (20 μl) was adsorbed onto the freeze-dried gelatin hydrogel, followed by leaving at 4 °C overnight to introduce ^{125}I into the amino groups of gelatin. The radioiodinated hydrogels were washed with DDW thoroughly to exclude the uncoupled, free ^{125}I molecules until the radioactivity of DDW equaled to the background level. Following the implantation into the back subcutis of mice, the hydrogels were taken out at each time-point to count the radioactivity remaining by the gamma counter. The experiment was independently performed for 3 samples per experimental group at each sampling point.

2.8. In vitro culture of macrophage-like and osteoblastic cells in the gelatin hydrogels incorporating triptolide-micelles and BMP-2

Mouse J774.1 macrophage-like cells were cultured in RPMI (Roswell Park Memorial Institute) 1640 medium supplemented with 10 vol% fetal bovine serum (FBS), and 100 U/ml penicillin and streptomycin at 37 °C in a 5% CO_2-95% air atmospheric condition. The medium was refreshed every other day. Suspension of J774.1 cells (10^6 cells/50 μl) was seeded into each hydrogel for 6 hr by the agitation seeding technique reported previously [36]. Further, 1

ml of medium was added into each cells-seeded hydrogel and the static culture was carried on. The total RNA of cells cultured in the hydrogels for 3 days was extracted by using RNeasy® fibrous tissue mini kit (Qiagen, Valencia, CA) according to the manufacturer's instruction. Reverse transcription reaction was performed with the SuperScript II First-Stand Synthesis System (Invitrogen Corporation, Ltd., CA). Real-time polymerase chain reaction (PCR) was performed on a Prism 7500 real time PCR thermal cycler (Applied Biosystems, Foster City, CA) from 10 ng of cDNA in a total volume of 25 μl containing Power SYBR Green PCR Master Mix (Applied Biosystems) and 10 μM of each primer (Table 1) to analyze the mRNA expression level of IL-6, TNF-α, and IL-10 genes. The reaction mixture was incubated for the initial denaturation at 95 °C for 10 min, followed by 40 PCR cycles. Each cycle consisted of the following two steps; 95 °C for 15 sec and 60 °C for 1 min. Each mRNA expression level was normalized by the expression level of glyceraldehyde-3-phosphate dehydrogenase (GAPDH) as an internal control. The experiment was independently performed for 3 samples per experimental group.

Mouse MC3T3-E1 osteoblast-like cells were cultured in alpha-modified Eagle minimal essential medium (α-MEM) supplemented with 10 vol% FBS, and 100 U/ml penicillin and streptomycin at 37 °C in a 5% CO_2-95% air atmospheric condition. The medium was refreshed every other day. Suspension of MC3T3-E1 cells (10^6 cells/50 μl) was seeded into the hydrogel and cultured as described previously. The medium was refreshed on day 3 and the activity of alkaline phosphatase (ALP) for cells cultured in the hydrogels for 7 days was assayed by the conventional *p*-nitrophenyl phosphate method [36]. The number of cells was determined by the fluorometric quantification of cellular DNA to normalize the ALP activity. The experiment was independently performed for 3 samples per experimental group.

2.9. In vivo bone defect experiment

All the animal experiments were performed according to the Institutional Guidance of Kyoto University on Animal Experimentation and under permission by animal experiment committee of Institute for frontier Medical Science, Kyoto University. A bone defect model of rat ulna was prepared to evaluate the bone regeneration after implantation of gelatin hydrogels incorporating 0, 2.5, 5 or 10 mg of triptolide-micelles and 5 μg of BMP-2. The surgery was made for 24 to 30-week-old male Wistar rats (400-500 g, n = 16) under standard sterile conditions according to the procedure previously reported [37]. Briefly, the rats were anesthetized with an intraperitoneal injection of pentobarbital sodium solution (40 mg/kg body weight). After shaving the hair and disinfection with 70 vol% ethanol, a longitudinal incision was made along the forearm skin of rats. The periosteum was incised circumferentially to approach to the ulna bone. A critical defect of 6 mm length was then created at the middle position of ulna bone by using a side-cutting diamond disk and a high-speed micromotor under an abundant irrigation with the sterile saline solution [38]. The hydrogel was implanted into the defect while the periosteum and overlying muscle were repositioned with an absorbable polydioxanone suture (Ethicon 5-0, NJ). Then, the wound was closed with a non-absorbable polypropylene suture (Ethicon 5-0, NJ). Each rat received the implantation of 2 hydrogels in both left and right of forearm's ulna. The experiment was independently performed for 4 samples per experimental group at each sampling point.

2.10. Evaluation of local inflammation responses at bone defects

Histogical and immunohistochemical stainings were performed to evaluate the local inflammation responses at the defects 3 days after the implantation of hydrogels incorporating 0, 2.5, 5 or 10 mg of triptolide-micelles and 5 μg of BMP-2. The hydrogel samples were collected, fixed with 3 wt% paraformaldehyde in PBS at 4 °C for 24 hr, decalcified with Plank-

Rychlo's Solution (0.3 M aluminium chloride, 3 vol% hydrochloric acid, and 5 vol% formic acid) at 4 °C for 4 days. The decalcification solution was changed every other day. After decalcification, the samples were neutralized with 5 wt% sodium sulfate solution at 4 °C for 24 hr, and washed repeatedly with DDW for further 24 hr. Then, the samples were embedded in Tissue-Tek OCT Compound (Sakura Finetek Inc., Tokyo, Japan), frozen on liquid nitrogen, and cryo-sectioned. The tissue sections (5 mm-thick) were stained with hematoxylin and eosin (H&E), Giemsa, and toluidine blue following the standard protocols to observe the infiltration of inflammatory cells, including lymphocytes, neutrophils, and mast cells. The images were taken under a microscope (AX80 Provis, Olympus Ltd., Tokyo, Japan) at 10X and 100X magnifications. The number of lymphocytes, neutrophils, and mast cells was counted from the images taken at 100X magnification randomly selected (30 images/experimental group).

For the immunohistochemical staining, the sections were washed with PBS, blocked with a normal goat serum at room temperature for 1 hr before incubation with a mouse anti-rat macrophage/dendritic cells monoclonal antibody (1:25, Clone no. RM-4, KT014, Cosmo Bio Co. Ltd., Tokyo, Japan) at room temperature for 1 hr. Then, the sections were washed with PBS and stained with an Alexa Flour 488-conjugated goat anti-mouse IgG (1:200, Invitrogen Corporation, Ltd., CA) at room temperature for 45 min. After washing, the sections were mounted with a Super Cryomounting Medium (SCMM, Leica Microsystems Co. Ltd., Tokyo, Japan). The fluorescence images were taken under a fluorescent microscope (Apotome, Imager.Z1, Carl Zeiss, Jena, Germany) at 10X magnification.

2.11. Evaluation of local gene expression of inflammatory cytokines at bone defects

The hydrogels implanted at the defects were taken out 3 days after implantation. The total RNA was extracted by using RNeasy fibrous tissue mini kit (Qiagen, Valencia, CA) according to the manufacturer's instruction. The RT-PCR assay was performed as described

previously to evaluate the mRNA expression level of IL-6, TNF-α, IL-10, NF-κB, and matrix metalloproteinase (MMP)-14 genes (Table 1) of cells infiltrated into the hydrogels implanted. Expression level of every group was reported as the value normalized to that of the sham group (the bone tissue collected from the rats which did not receive the operation and hydrogel implantation). Each mRNA level was normalized by the expression level of β-actin as an internal control. The experiment was independently performed for 4 samples per experimental group.

2.12. Evaluation of bone tissue regenerated at the defects

The bone tissue regenerated at the defect was evaluated 4 and 8 weeks later by radiological, micro-computed tomography (μCT), peripheral quantitative computed tomography (pQCT), and histological examinations. The radiological examination was performed under the soft x-ray machine (Hitex-100, Hitachi Ltd., Tokyo, Japan) at 56 kV and 2.5 mA for 20 s. Three-dimensional images of bone regenerated at the defects were visualized with the CT scans (X-RAY CT System, SMX-100CT-SV3 TYPE, Shimadzu Ltd., Kyoto, Japan). Samples were scanned over a fixed length of bone with a 20 mm sample holder at a resolution of 20 mm, energy of 30 kV, current of 25 mA, and exposure time of 300 ms. The 2-dimensional images were reconstructed and submitted to the VGStudio MAX 1.2 software (Volume Graphics GmbH, Heidelberg, Germany) for processing to produce the 3-dimensional images of bone regenerated. The bone mineral density (BMD) of whole cortical compartment of bone regenerated was analyzed by using a highly accurate multi-slice pQCT (XCT Research SAþ, Stratec Medizintechnik, GmbH, Pforzheim, Germany) at a resolution of 0.08 m voxel size and a threshold value of 267 mg/cm^3 with a scanning protocol of 3 slices with a thickness of 460 mm and a slice interval of 1 mm, at a defined distance. Analysis of the regional cortical BMD was carried out for each of 3 tomographic slices at a square region of interest (ROI)

generated. For the histological examination, the samples were fixed with 3 wt% paraformaldehyde in PBS at room temperature for 24 hr, decalcified and neutralized as described previously. Then, the samples were embedded in Tissue-Tek OCT Compound (Sakura Finetek Inc., Tokyo, Japan), and frozen on liquid nitrogen. The tissue sections (6 mm-thick) were cut at the center of samples, followed by staining with H&E to observe the bone tissue newly formed. The images were taken under a microscope (AX80 Provis, Olympus Ltd., Tokyo, Japan) at 10X magnification.

2.13. Statistical analysis

All the results were statistically analyzed by the unpaired student's t test and $p < 0.05$ was considered to be statistically significant. Data were expressed as the mean ± the standard deviation.

3. Results

3.1 The encapsulation efficiency and amount of triptolide incorporated in the micelles

The encapsulation efficiency of triptolide incorporated in the micelles was around 8.9 wt%. The amount of triptolide incorporated in the hydrogels (1 x 2 x 6 mm^3) incorporating 2.5, 5, and 10 mg of triptolide-micelles was 430±15, 705±38, and 1,268±230 ng, respectively.

3.2 Controlled release of triptolide and BMP-2 from gelatin hydrogels and hydrogel degradation

Figure 1A shows the *in vitro* time profiles of triptolide and BMP-2 release from gelatin hydrogels incorporating mixed triptolide-micelles and BMP-2. Triptolide was released from the gelatin hydrogels, irrespective of the dose incorporated. Every hydrogel released around 14%

of triptolide incorporated within the first day and the release became constant at 20% 5 days later. BMP-2 was gradually released from the hydrogels over 7 days. Within the first day, less BMP-2 release was observed for any gelatin hydrogel incorporating mixed triptolide-micelles and BMP-2 than for those incorporating BMP-2 without triptolide-micelles. However, thereafter, this difference became small and the percentage of BMP-2 released was around 30% 5 days later.

Figure 1B shows the *in vivo* time profiles of triptolide and BMP-2 release from gelatin hydrogels incorporating mixed triptolide-micelles and BMP-2 after implantation into the back subcutis of mice. A 60% initial burst of triptolide release was seen within the first day, irrespective of the dose incorporated. Triptolide was gradually released thereafter and around 20% of drug was remained in the hydrogels 7 days after implantation. On the first day, the percentage of BMP-2 released from every hydrogel was smaller (40-60%) than that of triptolide release. The incorporation of triptolide-micelles suppresed the initial burst of BMP-2 release from the gelatin hydrogels.

On the other hand, the gelatin hydrogels of release carriers were gradually degraded over 7 days and remained around 40% 7 days later (data not shown). Figures 2A and 2B show the remaining amount of the triptolide and BMP-2 incorporated in the gelatin hydrogels as a function of the hydrogels remaining, respectively. Irrespective of the dose incorporated, the time profile of both triptolide and BMP-2 releases were not always linearly correlated with that of the hydrogel degradation.

3.3 Expression level of inflammatory cytokines of J774.1 macrophage-like cells cultured in the hydrogels

Figure 3 shows the mRNA expression level of IL-6, TNF-α, and IL-10 genes of J774.1 macrophage-like cells cultured in the gelatin hydrogels incorporating mixed various doses of triptolide-micelles and BMP-2. The expression level of IL-6 and IL-10 genes was dose-dependently down-regulated with an increase in the amount of triptolide-micelles incorporated. On the other hand, no significant difference in the expression level of TNF-α gene was observed among the groups although the level seemed to increase with the increasing dose of triptolide-micelles.

3.4 Osteogenic differentiation of MC3T3-E1 osteoblastic cells cultured in the hydrogels

Figures 4A and B show the number and ALP activity of MC3T3-E1 cells cultured in the gelatin hydrogels incorporating mixed various doses of triptolide-micelles and BMP-2. No difference in the cell number was observed among the experimental groups. On the other hand, the ALP activity of cells cultured in the hydrogels incorporating every dose of triptolide-micelles and BMP-2 showed almost 3-time higher than that of the hydrogels incorporating BMP-2 without triptolide-micelles.

3.5 Local inflammation responses at the bone defect implanted with the hydrogels

Figures 5A-D show the histological and immunohistochemical images of inflammatory cells around the defects implanted with gelatin hydrogels incorporating mixed various doses of triptolide-micelles and BMP-2. H&E-stained sections indicated a significant inflammation response to the gelatin hydrogels incorporating BMP-2 without triptolide-micelles (Figure 5A). The accumulation of inflammatory cells was seen around this hydrogel implanted. In contrast, less number of inflammatory cells were observed for the hydrogels incorporating 2.5 and 5 mg

of triptolide-micelles and BMP-2. However, the hydrogels incorporating 10 mg of triptolide-micelles and BMP-2 showed the reverse inflammation, as observed by a highly accumulated inflammatory cells around the hydrogel. The similar phenomena were observed for Giemsa-stained sections (Figure 5B). In the toluidine blue-stained sections, a number of mast cells were present around the gelatin hydrogels incorporating BMP-2 without triptolide-micelles, whereas the cells infiltration was reduced for any hydrogel incorporating mixed triptolide-micelles and BMP-2 (Figure 5C). The infiltration of immunohistochemical-stained macrophages and dendritic cells was observed in the gelatin hydrogels incorporating BMP-2 without triptolide-micelles (Figure 5D). The infiltration was suppressed for the hydrogels incorporating mixed triptolide-micelles and BMP-2. Figure 5E shows the quantitative results of cells infiltration. The number of neutrophils and lymphocytes infiltrated was significantly reduced for the hydrogels incorporating 2.5 and 5 mg of triptolide-micelles and BMP-2. However, for the hydrogels incorporating 10 mg of triptolide-micelles and BMP-2, the number of neutrophils and lymphocytes was similar to that of the hydrogels incorporating BMP-2 without triptolide-micelles. On the other hand, the number of mast cells was signifficantly less for the hydrogels incorporating every dose of triptolide-micelles and BMP-2 than those incorporating BMP-2 without triptolide-micelles. A slightly increased cell number was seen for the hydrogels incorporating 10 mg of triptolide-micelles and BMP-2, compared with the hydrogels incorporating less amount of triptolide-micelles and BMP-2.

3.6 Expression of local inflammatory cytokines at the defect implanted with the hydrogels

Figure 6 shows the mRNA expression level of inflammatory cytokines of cells in the gelatin hydrogels 3 days after hydrogels implantation. The implantation of gelatin hydrogels incorporating BMP-2 without triptolide-micelles resulted in a highly up-regulated the expression of IL-6 (~900-fold) and TNF-α genes (~80-fold), while those incorporating

triptolide-micelles and BMP-2 dose-dependently down-regulated the expression. Despite the significantly down-regulated expression level, IL-6 and TNF-α expression of cells in hydrogels incorporating every dose of triptolide-micelles and BMP-2 remained higher than those of the sham group. The highly up-regulated expression of IL-10 gene was also observed for cells around the hydrogels incorporating BMP-2 without triptolide-micelles, although the expression level was approximately 2-fold decreased for the hydrogels incorporating every dose of triptolide-micelles and BMP-2. The tendency of NF-κB expression was rather similar to that of IL-6, TNF-α, and IL-10 genes for all the hydrogel groups, although they all were down-regulated from that of the sham group. The expression of MMP-14 gene in the hydrogels incorporating 2.5 and 5 mg of triptolide-micelles and BMP-2 was significantly reduced from that of other groups.

3.7 Bone regeneration at the defects implanted with the hydrogels

Figure 7 shows the qualitative and quantitative results of bone regeneration at the defects implanted with gelatin hydrogels incorporating triptolide-micelles and BMP-2. Soft x-ray images showed a slightly higher extent of bone regeneration at the defects implanted with the hydrogels incorporating 2.5 or 5 mg of triptolide-micelles and BMP-2 than that of other groups 4 and 8 weeks after implantation (Figure 7A). No bone regeneration was observed for the hydrogels incorporating 10 mg of triptolide-micelles and BMP-2 even at 8 weeks. The μCT results were in good accordance to those of x-ray examinations (Figure 7B). In the H&E-stained images, a high density of collagen tissue formation was observed for the hydrogels incorporating 2.5 and 5 mg of triptolide-micelles and BMP-2 4 weeks after implantation (Figure 7C). In contrast, the amount of collagen tissue formed was less for the hydrogels incorporating BMP-2 without or with 10 mg of triptolide-micelles incorporation. The quantitative results indicated a significantly enhanced BMD for the defects implanted with the

hydrogels incorporating 2.5 and 5 mg of triptolide-micelle and BMP-2, compared with the hydrogels incorporating BMP-2 without triptolide-micelles (Figure 7D). For the hydrogels incorporating 10 mg of triptolide-micelles and BMP-2, the BMD value was not obtained because of no bone regeneration.

4. Discussion

The initial inflammation is recognized to be a crucial stage for the subsequent reparative and remodeling processes of bone healing. It is well known that excessive local inflammation characterized by the over-expression of pro-inflammatory cytokines, particularly that induced by the surgical procedure or the material implantation, often delays the process of tissue regeneration [4-6,9-11]. Thus, it is important to consider the inflammation modulation to maintain or enhance the capability of tissue regeneration. In this study, it is hypothesized that the enhanced tissue regeneration would be achieved under a condition of inflammation suppression in the inflammation-induced model. Bone regeneration was evaluated for a critical-sized defect implanted with hydrogels incorporating immunosuppressive drug and BMP-2 to prove this hypothesis. The inflammation was artificially induced by the surgical operation and the implantation of foreign-body hydrogels incorporating BMP-2 of a foreign protein. The combined effects would result in a highly local inflammation around the defect area, as can be confirmed by a significant up-regulated expression of pro- and anti-inflammatory cytokines, compared with that of sham group (Figure 6). Furthermore, in this study, middle-aged rats (24 to 30-week-old) were used to prepare the defect model instead of young rats (~12-week-old) in order to make use of stronger activation of pro-inflammatory cytokines [39]. Another challenging point of this study is to experimentally confirm whether or not the bone regeneration may be enhanced by the inflammation modulation for aged rats.

As the controlled release carrier, the gelatin hydrogel was selected because it is non-cytotoxic, biodegradable, easy to process, inexpensive, and has been used clinically. Our previous researches demonstrated that gelatin hydrogels could release various kinds of growth factors, such as basic fibroblast growth factors (bFGF) [28], BMP-2 [25-27], and transforming growth factor-β1 (TGF- β1) [29], the nucleic acids of plasmid DNA [30] and small interfering RNA [31] or low molecular-weight drugs [32,33]. In this study, triptolide of a water-insoluble drug can be released in a controlled fashion from the gelatin hydrogels by utilizing the micelle formation. The triptolide release can modulate the extent of local inflammation. The doses of triptolide incorporated were selected based on the effective dose demonstrated by other researches [40-42]. The *in vitro* release of triptolide-micelles and BMP-2 from the hydrogels showed a saturated pattern within 7 days (Figure 1A). This saturation is due to the complete incorporation of drug in the hydrogel matrix. In the *in vitro* system without any degradation enzymes of hydrogels, the drug incorporated is not released following the initial diffusional release of non-incorporated drug. On the other hand, both the triptolide and BMP-2 were released simultaneously from the hydrogels over 7 days *in vivo* (Figure 1B). It is possible that the presence of degradation enzymes accelerated the hydrogel degradation to make water-soluble gelatin fragments, resulting in the drug release in the *in vivo* system. It is important to note that most of triptolide incorporated was released within the initial inflammation period (< 7 days) which is a target timing of this study. The initial release of BMP-2 from the hydrogels co-incorporating triptolide-micelles was slightly suppressed compared with the hydrogels without triptolide-micelles incorporation, while the release of triptolide was not affected by the BMP-2 incorporation for both the *in vitro* and *in vivo* systems. This phenomenon can be explained by the viewpoint of interaction forces between the two molecules incorporated in the hydrogel carriers. Triptolide, BMP-2, and the gelatin have a co-interaction in the matrix of hydrogels. It is possible that the BMP-2 interacts not only with the gelatin of hydrogel matrix,

but also with the triptolide-micelles. As the result, the double interaction would suppress the BMP-2 release. Several studies have also reported on difference in the release behavior between the two molecules incorporated in one carrier [43,44]. It is found that the release of indomethacin from a heparin-conjugated polymeric micelle was suppressed by the combination of basic fibroblast growth factor (bFGF) whereas the indomethacin combination did not affect the profile of bFGF release [43].

The expression of IL-6 and IL-10 by J774.1 macrophage-like cells was dose-dependently down-regulated when cultured in the hydrogels incorporating mixed triptolide-micelles and BMP-2 (Figure 3). This experimentally confirms the potential activity of triptolide incorporated *in vitro*. An increase in the ALP activity, an early marker of osteogenic differentiation, was observed for MC3T3-E1 osteoblastic cells cultured in the hydrogels incorporating triptolide-micelles and BMP-2 (Figure 4). The reason for the enhanced osteogenic differentiation of osteoblastic cells by the co-incorporation of triptolide-micelles and BMP-2 in the hydrogels is not clear at present. To our knowledge, the effect of triptolide on osteogenic differentiation of cells has not been reported elsewhere. It is hypothesized that the suppression of pro-inflammatory cytokines of osteoblastic cells by the triptolide incorporation (data not shown) would be one of the reasons to modify the subsequent signaling cascade of BMP-2-induced osteogenic differentiation [9,11].

The inflammation suppression effect of hydrogels incorporating triptolide-micelles and BMP-2 was further confirmed by the local histology and gene expression level of inflammatory cytokines after implantation in the bone defects 3 days (Figures 5 and 6). A number of neutrophils, lymphocytes, mast cells, macrophages, and dendritic cells were accumulated around the defects implanted with the hydrogels incorporating BMP-2 without triptolide-micelles. This would be the combined effects of the surgery, foreign body hydrogel, and BMP-

2 to induce the local inflammation. In Figure 5, the reduced number and accumulation of inflammatory cells around the defects implanted with the hydrogels incorporating 2.5 and 5 mg of triptolide-micelles and BMP-2 indicated the suppressed inflammation responses at the bone defects. The similar reduced number of inflammatory cells by triptolide was also reported by other research groups although the triptolide was delivered via different routes, such as an oral administration, intraperitoneal injection or medium supply [16,17,23,24,45-47].

Liu *et al.* demonstrated that triptolide significantly impaired dendritic cells-mediated chemoattraction of neutrophils and T-lyphocytes both *in vitro* and *in vivo* by suppressing the production of macrophage inflammatory protein (MIP)-1α, MIP-1β, and interferon-c-inducible protein (IP)-10 in response to lipopolysaccharide (LPS) [17]. Yang *et al.* reported that triptolide added into the culture medium suppressed mitogen-induced T-lymphocytes proliferation by inducing their apoptotic death and by inhibiting IL-2 receptor expression [16,46]. Triptolide also effectively inhibited the growth of both human and murine mast cells by the inhibition of KIT (transmembrane receptor tyrosine kinase of the type III subgroup) mRNA levels and the levels of phosphorylated and total Stat3, Akt, and Erk1/2, downstream targets of KIT [47]. In addition, triptolide suppressed the differentiation of immature human monocytes to macrophages and inhibited the migration of dendritic cells into tissues by inhibiting the expression of chemokine (C-C motif) receptor (CCR)-7 and cyclooxygenase (COX)-2 through phosphoinositide 3-kinase (PI3-K)/Akt and NF-κB pathways [23,24]. However, it is important to note that the triptolide release from the hydrogels incorporating 2.5 and 5 mg of triptolide-micelles and BMP-2 only suppressed, but not completely diminished the local inflammation. The reduced inflammation would be possibly sufficient to initiate the subsequent regeneration processes.

In term of gene expression of pro- (IL-6 and TNF-α) and anti-inflammatiory cytokines (IL-10), the implantation of gelatin hydrogels incorporating BMP-2 without triptolide-micelles induced a significant inflammation response at the defect site (Figure 6). However, the expression of IL-6 and TNF-α was suppressed by the triptolide incorporated in the hydrogels in a dose-dependent manner (Figure 6), although the up-regulation was still observed when compared with that of the sham group. This finding confirms that triptolide has a potential effect on the suppression of pro-inflammatory cytokines, which is reported by other groups [48]. IL-10, as an anti-inflammatory cytokine inhibiting the release of pro-inflammatory cytokines and subsequent preventing tissue damage [49], also showed the up-regulated expression similarly to that of pro-inflammatory cytokines (Figure 6). It is understandable that the highest up-regulation of anti-inflammatory cytokines would be required for the highest expression of pro-inflammatory cytokine of the hydrogels incorporating BMP-2 without triptolide-micelles in order to counter balance the inflammation responses [50,51], while the expression of IL-10 became lower for the hydrogels incorporating triptolide-micelles and BMP-2 where the inflammation was reduced.

The expression of NF-κB, a transcription factor controlling the expression of many genes involved in biological cascades, also corresponded to that of pro- and anti-inflammatory cytokines. The hydrogels incorporating triptolide-micelles and BMP-2 suppressed the NF-κB expression, compared with that of the hydrogels incorporating BMP-2 without triptolide-micelles. This was possibly due to a direct regulatory role of triptolide to suppress the NF-κB transcriptional signal-mediated inflammation [52,53]. However, it is known that the NF-κB transcription is regulated by other biological events, such as apoptosis, metastasis, carcinoma or cell survival in addition to the inflammation [54,55]. This may partially explain the reason

why the NF-κB expression was down-regulated under the inflammation-induced condition of every hydrogel group in this study, compared with that of the sham group.

The overall effect of inflammation suppression induced by the hydrogels incorporating 2.5 and 5 mg of triptolide-micelles and BMP-2 may contribute to the less tissue damage and consequently enhanced the bone regeneration. An enhanced tissue repair is reported by the neutralizing IL-6 signal [56]. Mukaino *et al.* demonstrated that the repair of spinal cord injury can be promoted by the administration of an anti-IL-6 receptor antibody immediately after injury [56]. This effect was explained by the switch of the central player in the post-traumatic inflammation, from hematogenous macrophages to resident microglia, accompanied by alterations in the expression of relevant cytokines within the injured spinal cord.

The hydrogels incorporating 10 mg of triptolide-micelles and BMP-2 showed the strong inflammation (Figure 5E). This inflammation was also confirmed by a separated experimental model. The hydrogels incorporating various doses of triptolide-micelles without BMP-2 were implanted subcutaneously in the LPS-induced mice. The implantation of hydrogels incorporating 10 mg of triptolide-micelles substantially up-regulated IL-6 and TNF-α expression while those mRNA genes and the number of neutrophils and macrophages were significantly suppressed for the hydrogels incorporating 5 mg of triptolide-micelles, as analyzed by real-time PCR (Figure S1) and flow cytometry (Figure S2). The inflammation-induction responses of triptolide at high dose were also reported by Xu *et al.* [57]. The effective dose of triptolide was nearly equal to its toxic dose and the reversible skin irritation was observed on the animals given at the high dose of triptolide. On the other hand, in this study, macrophages and dendritic cells seemed to be suppressed by every dose of triptolide-micelles incorporated and the inflammation-induced responses were not observed even at the

high dose (Figure 5D). The reason is still unclear at present. However, the controlled release of triptolide may influence the dose-dependent response.

Considering the gene expression of inflammatory cytokines, no higher expression of pro-inflammatory cytokines was observed even for the hydrogels incorporating 10 mg of triptolide-micelles and BMP-2 (Figure 5). This is not well corresponded to the increased number of inflammatory observed histologically (Figure 5). It may be that triptolide plays a direct role in the inhibition of IL-6 and TNF-α production by inflammatory cells through the suppression of NF-κB signal [52,53]. Thus, it is possible that the suppressed IL-6 and TNF-α expression was remained even though the number of some inflammatory cells increased. Interestingly, no bone regeneration was observed at the defects implanted with the hydrogels incorporating 10 mg of triptolide-micelles and BMP-2. It is supposed that a significant local inflammation would hinder the regeneration processes. In addition, IL-6 and TNF-α expression almost completely diminished by the hydrogels incorporating 10 mg of triptolide-micelles and BMP-2 would not facilitate the following biological sequences.

MMP-14 is of the matrix metalloproteinase (MMP) family involved in the breakdown and turnover of extracellular matrix (ECM) [58]. It is reported that the expression level of MMP family including MMP-14 was induced to breakdown the ECM during tissue inflammation and subsequently down-regulated to diminish matrix degradation thereby promoting matrix deposition to achieve reconstitution of the tissue repair process [59]. In this study, the MMP-14 expression was up-regulated only for the hydrogels incorporating BMP-2 without triptolide-micelles, while the hydrogels incorporating 2.5 and 5 mg of triptolide-micelles and BMP-2 showed a significantly down-regulation. This may suggest that the tissue around the defects implanted with the hydrogels incorporating 2.5 and 5 mg of triptolide-micelles and BMP-2 would be possibly in the earlier turnover phase for tissue repair than that

of other two hydrogel groups. As a result, the bone tissue was regenerated in the defects implanted with the hydrogels incorporating 2.5 and 5 mg of triptolide-micelles and BMP-2 to a high extent even at the earlier time-point (4 weeks) post-operation (Figures 7A and C).

Some potential osteoinductive molecules, such as dexamethasone and 1,25-dihydroxyvitamin D3, are also known for their anti-inflammatory function [60-63]. Their underlying mechanism to promote bone regeneration may be explained in terms of the inflammation suppression effect, in addition to the direct regulatory role on the osteogenesis cascades. The present study demonstrates that a proper condition of inflammation suppression is one of the main factors contributing to the enhanced BMP-2-induced bone regeneration. The reduced number of inflammatory cells as well as the suppressed expression of pro-inflammatory cytokines were achieved by the controlled co-release of triptolide and BMP-2 from the gelatin hydrogels.

5. Conclusion

The effect of local inflammation suppression on the bone regeneration was evaluated by the controlled co-release of immunosuppressive triptolide and BMP-2 from the gelatin hydrogels. The local inflammation responses were significantly reduced at the defects implanted with the hydrogels incorporating mixed 2.5 or 5 mg of triptolide-micelles and BMP-2, and the subsequent bone regeneration was enhanced thereat, compared with the hydrogels incorporating BMP-2 without triptolide-micelles. On the other hand, the implantation of hydrogels incorporating mixed 10 mg of triptolide-micelles and BMP-2 highly induced inflammation and inhibited the bone regeneration. Therefore, the proper local modulation of inflammation responses is a promising way to achieve the enhanced bone regeneration.

Acknowledgements

The research was supported by a grant from Japan Society for the Promotion of Science (JSPS). We gratefully thank Associate Professor Masaya Yamamoto, Dr. Makoto Matsui, Dr. Hiroshi Kohara, Dr. Tatsuya Okamoto, Dr. Hiromitsu Negoro, Dr. Atsuko Miyazawa, and Mr. Takashi Saito for their insightful discussion and technical assistance. We also acknowledged Professor Takayoshi Nakano and Assistant Professor Takuya Ishimoto for their assistance on pQCT analysis at the Graduate School of Engineering, Osaka University.

References

[1] Wan C, He Q, Li G. Allogenic peripheral blood derived mesenchymal stem cells (MSCs) enhance bone regeneration in rabbit ulna critical-sized bone defect model. J Orthop Res 2006;24:610-8.

[2] Kuznetsov SA, Mankani MH, Gronthos S, Satomura K, Bianco P, Robey PG. Circulating skeletal stem cells. J Cell Biol 2001;153:1133-9.

[3] Rundle CH, Wang H, Yu H, Chadwick RB, Davis EI, Wergedal JE, et al. Microarray analysis of gene expression during the inflammation and endochondral bone formation stages of rat femur fracture repair. Bone 2006;38:521-9.

[4] Cooper PR, Takahashi Y, Graham LW, Simon S, Imazato S, Smith AJ. Inflammation-regeneration interplay in the dentine–pulp complex. J Dent 2010;38:687-97.

[5] Goertz O, Ring A, Buschhaus B, Hirsch T, Daigeler A, Steinstraesser L, et al. Influence of anti-inflammatory and vasoactive drugs on microcirculation and angiogenesis after burn in mice. Burns 2011;37:656-64.

[6] Corsetti G, Antona GD, Dioguardi FS, Rezzani R. Topical application of dressing with amino acids improves cutaneous wound healing in aged rats. Acta histochem 2010;112:497-507.

[7] Mountziaris PM, Mikos AG. Modulation of the inflammatory response for enhanced bone tissue regeneration. Tissue Eng Part B 2008;14:179-86.

[8] Gerstenfeld LC, Cho TJ, Kon T, Aizawa T, Tsay A, Fitch J, et al. Impaired fracture healing in the absence of TNF-a signaling: the role of TNF-a in endochondral cartilage resorption. J Bone Miner Res 2003;18:1584-92.

[9] Lacey DC, Simmons PJ, Graves SE, Hamilton JA. Proinflammatory cytokines inhibit osteogenic differentiation from stem cells: implications for bone repair during inflammation. Osteoarthr Cartilage 2009;17:735-42.

[10] Wu G, Liu Y, Iizuka T, Hunziker EB. The effect of a slow mode of BMP-2 delivery on the inflammatory response provoked by bone-defect-filling polymeric scaffolds. Biomaterials 2010;31:7485-93.

[11] Kim SE, Song SH, Yun YP, Choi BJ, Kwon IK, Bae MS, et al. The effect of immobilization of heparin and bone morphogenic protein-2 (BMP-2) to titanium surfaces on inflammation and osteoblast function. Biomaterials 2011;32:366-73.

[12] Nyangoga H, Aguado E, Goyenvalle E, Baslé MF, Chappard D. A non-steroidal anti-inflammatory drug (ketoprofen) does not delay b-TCP bone graft healing. Acta Biomater 2010;6:3310-7.

[13] Penga LH, Ko CH, Siu SW, Koon CM, Yue GL, Cheng WH, et al. In vitro & in vivo assessment of a herbal formula used topically for bone fracture treatment. J Ethnopharmacol 2010;131:282-9.

[14] Qiu D, Zhao G, Aoki Y, Shi L, Uyei A, Nazarian S, et al. Immunosuppressant PG490 (triptolide) inhibits T-cell interleukin-2 expression at the level of purine-box/nuclear factor of activated T-cells and NF-KappaB transcriptional activation. J Biol Chem 1999;274:13443-50.

[15] Krakauer T, Chen X, Howard OM, Young HA. Triptolide attenuates endotoxin- and staphylococcal exotoxin-induced T cell proliferation and production of cytokines and chemokines. Immunopharm Immunot 2005;27:53-66.

[16] Yang Y, Liu Z, Tolosa E, Yang J, Li L. Triptolide induces apoptotic death of T lymphocyte, Immunopharmacology 1998;40:139-49.

[17] Liu Q, Chen T, Chen G, Li N, Wang J, Ma P, et al. Immunosuppressant triptolide inhibits dendritic cell-mediated chemoattraction of neutrophils and T cells through inhibiting Stat3 phosphorylation and NF-kappaB activation. Biochem Bioph Res Co 2006;345:1122-30.

[18] Wang J, Xu R, Jin R, Chen Z, Fidler JM. Immunosuppressive activity of the Chinese medicinal plant Tripterygium wilfordii. I. Prolongation of rat cardiac and renal allograft survival by the PG27 extract and immunosuppressive synergy in combination therapy with cyclosporine. Transplantation 2000;70:447-55.

[19] Fidler JM, Ku GY, Piazza D, Xu R, Jin R, Chen Z. Immunosuppressive activity of the Chinese medicinal plant Tripterygium wilfordii. III. Suppression of graft-versus-host disease in murine allogeneic bone marrow transplantation by the PG27 extract. Transplantation 2002;74:445-57.

[20] Zheng J. Screening of active anti-inflammatory, immunosuppressive and antifertility components of Tripterygium wilfordii: III. A comparison of the anti-inflammatory and immunosuppressive activities of 7 diterpene lactone epoxide compounds in vivo. Acta Acad Med Sin 1991;13:391-7.

[21] Gu WZ, Chen R, Brandwein S, McAlpine J, Burres N. Isolation, purification, and characterization of immunosuppressive compounds from tripterygium: triptolide and tripdiolide. Int J Immunopharmaco 1995;17:351-6.

[22] Wei X, Gong J, Zhu J, Wang P, Li N, Zhu W, et al. The suppressive effect of triptolide on chronic colitis and TNF-α/TNFR2 signal pathway in interleukin-10 deficient mice. Clin Immunol 2008;129:211-8.

[23] Zhu KJ, Shen QY, Cheng H, Mao XH, Lao LM, Hao GL. Triptolide affects the differentiation, maturation and function of human dendritic cells, Int Immunopharmacol 2005;5:1415-26.

[24] Liu Q, Chen T, Chen G, Shu X, Sun A, Ma P, et al. Triptolide impairs dendritic cell migration by inhibiting CCR7 and COX-2 expression through PI3-K/Akt and NF-κB pathways. Mol Immunol 2007;44:2686-96.

[25] Yamamoto M, Takahashi Y, Tabata Y. Controlled release by biodegradable hydrogyels enhances the ectopic bone formation of bone morphogenetic protein. Biomaterials 2003;24:4375-83.

[26] Kimura Y, Miyazaki N, Hayashi N, Otsuru S, Tamai K, Kaneda Y, et al. Controlled release of bone morphogenetic protein-2 enhances recruitment of osteogenic progenitor cells for de novo generation of bone tissue. Tissue Eng Part A 2010;16:1263-70.

[27] Ratanavaraporn J, Furuya H, Kohara H, Tabata Y. Synergistic effects of the dual release of stromal cell-derived factor-1 and bone morphogenetic protein-2 from hydrogels on bone regeneration. Biomaterials 2011;32:2797-811.

[28] Tabata Y, Hijikata S, Ikada Y. Enhanced vascularization and tissue granulation by basic fibroblast growth factor impregnated in gelatin hydrogels. J Control Release 1994;31:189-99.

[29] Yamamoto M, Tabata Y, Hong L, Miyamoto S, Hashimoto N, Ikada Y. Bone regeneration by transforming growth factor beta1 released from a biodegradable hydrogel. J Control Release 2000;64:133-42.

[30] Kido Y, Jo J, Tabata Y. A gene transfection for rat mesenchymal stromal cells in biodegradable gelatin scaffolds containing cationized polysaccharides. Biomaterials 2011;32:919-25.

[31] Nakamura M, Jo J, Tabata Y, Ishikawa O. Controlled delivery of T-box 21 siRNA ameliorates autoimmune alopecia (alopecia areata) in C3H/HeJ mouse model. Am J Pathol 2008;172:650-8.

[32] Konishi M, Tabata Y, Kariya M, Hosseinkhani H, Suzuki A, Fukuhara K, et al. In vivo anti-tumor effect of dual release of cisplatin and adriamycin from biodegradable gelatin hydrogel. J Control Release 2005;103:7-19.

[33] Tanigo T, Takaoka R, Tabata Y. Sustained release of water-insoluble simvastatin from biodegradable hydrogel augments bone regeneration. J Control Release 2010;143:201-6.

[34] Ozeki M, Tabata Y. In vivo degradability of hydrogels prepared from different gelatins by various cross-linking methods. J Biomater Sci Polym Ed 2005;16:549-61.

[35] Kimura Y, Tabata Y. Controlled release of stromal cell-derived factor-1 from gelatin hydrogels enhances angiogenesis. J Biomater Sci Polym Ed 2010;21:37-51.

[36] Takahashi Y, Yamamoto M, Tabata Y. Osteogenic differentiation of mesenchymal stem cells in biodegradable sponges composed of gelatin and β-tricalcium phosphate. Biomaterials 2005;26:3587-96.

[37] Virk MS, Conduah A, Park SH, Liu N, Sugiyama O, Cuomo A, et al. Influence of short-term adenoviral vector and prolonged lentiviral vector mediated bone morphogenetic protein-2 expression on the quality of bone repair in a rat femoral defect model. Bone 2008;42:921-31.

[38] Hollinger JO, Kleinschmidt JC. The critical size defect as an experimental model to test bone repair materials. J Craniofac Surg 1990;1:60-8.

[39] Tang B, Matsuda T, Akira S, Nagata N, Ikehara S, Hirano T, et al. Age-associated increase in interleukin 6 in MRL/lpr mice. Int Immunol 1991;3:273-8.

[40] Chen H, Chang X, Weng T, Zhao X, Gao Z, Yang Y, et al. A study of microemulsion systems for transdermal delivery of triptolide. J Control Release 2004;98:427-36.

[41] Liu M, Dong J, Yang Y, Yang X, Xu H. Anti-inflammatory effects of triptolide loaded poly(d,l-lactic acid) nanoparticles on adjuvant-induced arthritis in rats. J Ethnopharmacol 2005;97:219-25.

[42] Lin N, Liu C, Xiao C, Jia H, Imada K, Wu H, et al. Triptolide, a diterpenoid triepoxide, suppresses inflammation and cartilage destruction in collagen-induced arthritis mice. Biochem Pharmacol 2007;73:136-46.

[43] Lee JS, Bae JW, Joung YK, Lee SJ, Han DK, Park KD. Controlled dual release of basic fibroblast growth factor and indomethacin from heparin-conjugated polymeric micelle. Int J Pharm 2008;346:57-63.

[44] Holland TA, Tabata Y, Mikos AG. Dual growth factor delivery from degradable oligo (poly(ethylene glycol) fumarate) hydrogel scaffolds for cartilage tissue engineering. J Control Release 2005;10:111-25.

[45] Hoyle GW, Hoyle CI, Chen J, Chang W, Williams RW, Rando RJ. Identification of triptolide, a natural diterpenoid compound, as an inhibitor of lung inflammation. Am J Physiol Lung Cell Mol Physiol 2010;298:L830–6.

[46] Yang SX, Xie SS, Gao HL, Ma DL, Long ZZ. Triptolide suppresses T-lymphocyte proliferation by inhibiting interleukin-2 receptor expression, but spares interleukin-2 production and mRNA expression. Int J Immunopharmaco 1994;16:895-904.

[47] Jin Y, Chen Q, Shi X, Lu Z, Cheng C, Lai Y, et al. Activity of triptolide against human mast cells harboring the kinase domain mutant KIT. Cancer Sci 2009;100:1335-43.

[48] Ho JC, Tipoe G, Zheng L, Leung TM, Tsang KWT, Shum DKY, et al. In vitro study of regulation of IL-6 production in bronchiectasis. Resp Med 2004;98:334-41.

[49] Howard M, O'Garra A. Biological properties of interleukin 10. J Clin Immunol 1992;12:239-47.

[50] Lesur I, Textoris J, Loriod B, Courbon C, Garcia S, Leone M. Gene expression profiles characterize inflammation stages in the acute lung injury in mice. Plos One 2010;5:1-14.

[51] Okamoto T, Saito T, Tabata Y, Uemoto S. Immunological tolerance in a mouse model of immune-mediated liver injury induced by 16,16 dimethyl PGE2 and PGE2-containing nanoscale hydrogels, Biomaterials 2011;32:4925-35.

[52] Jun LY, Jie J, Gui WY. Triptolide inhibits transcription factor NF-kappaB and induces apoptosis of multiple myeloma cells. Leukemia Res 2005;29:99-105.

[53] Dai YQ, Jin DZ, Zhu XZ, Lei DL. Triptolide inhibits COX-2 expression via NF-kappa B pathway in astrocytes. Neurosci Res 2006;55:154-60.

[54] Karin M, Greten FR. NF-κB: Linking inflammation and immunity to cancer development and progression. Nat Rev 2005;5:749-59.

[55] Yong-tang W, Xiu-min L, Ying Y, Yan-hong Y, Jie G. Expression of NF-κB in schwann cells and its effect on motor neuron apoptosis in spinal cord following sciatic nerves injury in rats. J Med Colleges PLA 2007;22:92-6.

[56] Mukaino M, Nakamura M, Yamada O, Okada S, Morikawa S, Renault-Mihara F, et al. Anti-IL-6-receptor antibody promotes repair of spinal cord injury by inducing microglia-dominant inflammation. Exp Neurol 2010;224:403-14.

[57] Xu L, Pan J, Chen Q, Yu Q, Chen H, Xu H, et al. In vivo evaluation of the safety of triptolide-loaded hydrogel-thickened microemulsion. Food Chem Toxicol 2008;46:3792-9.

[58] Bai S, Thummel R, Godwin AR, Nagase H, Itoh Y, Li L, et al. Matrix metalloproteinase expression and function during fin regeneration in zebrafish: Analysis of MT1-MMP, MMP2 and TIMP2. Matrix Biol 2005;24:247-60.

[59] Knittel T, Mehde M, Grundmann A, Saile B, Scharf JG, Ramadori G. Expression of matrix metalloproteinases and their inhibitors during hepatic tissue repair in the rat. Histochem Cell Biol 2000;113:443-53.

[60] Katoh N, Ito T. Inhibition by dexamethasone of interleukin-ll3 and interleukin-6 expression in alveolar macrophages from cows. Res Vet Sci 1995;59:41-4.

[61] Mountziaris PM, Tzouanas SN, Mikos AG. Dose effect of tumor necrosis factor-α on in vitro osteogenic differentiation of mesenchymal stem cells on biodegradable polymeric microfiber scaffolds. Biomaterials 2010;31:1666-75.

[62] Giulietti A, Etten EV, Overbergh L, Stoffels K, Bouillon R, Mathieu C. Monocytes from type 2 diabetic patients have a pro-inflammatory profile: 1,25-Dihydroxyvitamin D3 works as anti-inflammatory. Diabetes Res Clin Pr 2007;77:47-57.

[63] Suzuki Y, Ichiyama T, Ohsaki A, Hasegawa S, Shiraishi M, Furukawa S. Anti-inflammatory effect of 1α,25-dihydroxyvitamin D3 in human coronary arterial endothelial cells: Implication for the treatment of Kawasaki disease. J Steroid Biochem 2009;113:134-8.

Figure captions

Figure 1 (A) *In vitro* release profiles of triptolide (solid marks) and BMP-2 (open marks) from gelatin hydrogels incorporating mixed triptolide-micelles and ^{125}I-labeled BMP-2 in PBS at 37 °C. (B) *In vivo* release profiles of triptolide (solid marks) and BMP-2 (open marks) from gelatin hydrogels incorporating mixed triptolide-micelles and ^{125}I-labeled BMP-2 after implantation into the back subcutis of mice. The amount of triptolide-micelles incorporated was 0 (◯), 2.5 (▲,△), 5 (◆,◇) or 10 mg (■,□) while that of BMP-2 was 5 μg.

Figure 2 (A) Relationship of the remaining amount between the triptolide incorporated in hydrogels and the hydrogels of release carriers after implantation of gelatin hydrogels incorporating mixed 2.5 (▲), 5 (◆) or 10 mg of triptolide-micelles (■) and 5 μg of BMP-2 into the back subcutis of mice. (B) Relationship of the remaining radioactivity between the ^{125}I-labeled BMP-2 incorporated in hydrogels and the ^{125}I-labeled hydrogels of release carriers after implantation of gelatin hydrogels incorporating mixed 0 (◯), 2.5 (△), 5 (◇) or 10 mg of triptolide-micelles (□) and 5 μg of BMP-2 into the back subcutis of mice.

Figure 3 Gene expression of IL-6, TNF-α, and IL-10 cytokines of J774.1 macrophage-like cells 3 days after cultured in gelatin hydrogels incorporating mixed various amounts of triptolide-micelles and 500 ng of BMP-2. *p, < 0.05; significant against the value of gelatin hydrogels incorporating BMP-2 without triptolide-micelles, †p, < 0.05; significant between the two experimental groups.

Figure 4 (A) Number and (B) ALP activity of MC3T3-E1 cells 7 days after cultured in gelatin hydrogels incorporating mixed various amounts of triptolide-micelles and 500 ng of BMP-2. *p, < 0.05; significant against the value of gelatin hydrogels incorporating BMP-2 without triptolide-micelles.

Figure 5 Histological and immunohistochemical (IHC) images of inflammatory cells at the bone defects 3 days after implantation of gelatin hydrogels incorporating mixed various amounts of triptolide-micelles and 5 μg of BMP-2: (A) H&E, (B) Giemsa or (C) toluidine blue stainings, and (D) IHC images of macrophages and dendritic cells (scale bar = 100 μm, arrow: inflammatory cells). (E) Number of neutrophils, lymphocytes, and mast cells at the bone defect 3 days after the hydrogels implantation. *p, < 0.05; significant against the value of gelatin hydrogels incorporating BMP-2 without triptolide-micelles, †p, < 0.05; significant between the two experimental groups.

Figure 6 Gene expression of IL-6, TNF-α, IL-10, NF-κB, and MMP-14 of cells in gelatin hydrogels incorporating mixed various amounts of triptolide-micelles and 5 μg of BMP-2 3 days after implantation into the bone defects. *p, < 0.05; significant against the value of sham group, †, p < 0.05; significant between the two experimental groups.

Figure 7 (A) Soft x-ray images of bone regenerated at the defects 4 (left) and 8 weeks (right) after implantation of gelatin hydrogels incorporating mixed various amounts of triptolide-micelles and 5 μg of BMP-2. (B) μCT images of bone regenerated at the defects 8 weeks after implantation of the same hydrogels. (C) H&E images of bone regenerated at the defects 8 weeks after implantation of the same hydrogels (scale bar = 100 μm, C: collagen newly formed, S: scaffolding hydrogel). (D) Bone mineral density of bone regenerated at the defects 8 weeks after implantation of the same hydrogels. *p, < 0.05; significant against the value of gelatin hydrogels incorporating BMP-2 without triptolide-micelles.

Figure S1 Gene expression of IL-6 and TNF-α of cells in gelatin hydrogels incorporating mixed various amounts of triptolide-micelles 3 days after implantation into the back subcutis of LPS-induced mice. *p, < 0.05; significant against the value of gelatin hydrogels without triptolide-micelles.

Figure S2 Fraction of CD11b- and F4/80-positive (macrophages) and CD11b- and Ly6G-positive cells (neutrophils) in gelatin hydrogels incorporating 5 and 10 mg of triptolide-micelles 3 days after implantation into the back subcutis of LPS-induced mice.*p, < 0.05; significant between the two experimental groups.

Table 1. Primers used in quantitative real-time PCR analysis.

m RNA	Forward	Reverse
In vitro mouse cell line		
IL-6	5´-TGATGGATGCTACCAAACTGG-3´	5´-TTCATGTACTCCAGGTAGCTATGG-3´
TNF-α	5´-TCTTCTCATTCCTGCTTGTGG-3´	5´-GGTCTGGGCCATAGAACTGA-3´
IL-10	5´-CAGAGCCACATGCTCCTAGA-3´	5´-GTCCAGCTGGTCCTTTGTTT-3´
GAPDH	5´-TGTTGAAGTCACAGGAGACAAACCT-3´	5´-AACCTGCCAAGTATGATGACATCA-3´
In vivo rat model		
IL-6	5´-CCCTTCAGGAACAGCTATGAA-3´	5´-ACAACATCAGTCCCAAGAAGG-3´
TNF-α	5´-TGAACTTCGGGGTGATCG-3´	5´-GGGCTTGTCACTCGAGTTTT-3´
NF-κB	5´-ACTGCTCAGGCCCACTTG-3´	5´-TGTCATTATCTCGGAGCTCATCT-3´
IL-10	5´-AGTGGAGCAGGTGAAGAATGA-3´	5´-TCATGGCCTTGTAGACACCTT-3´
OPG	5´-TGAGGTTTCCAGAGGACCAC-3´	5´-GGAAAGGTTTCCTGGGTTGT-3´
IFN-γ	5´-TTTTGCAGCTCTGCCTCAT-3´	5´-AGCATCCATGCTACTTGAGTTAAA-3´
MMP-14	5´-AACTTCGTGTTGCCTGATGA-3´	5´-TTTGTGGGTGACCCTGACTT-3´
β-actin	5´-CCCGCGAGTACAACCTTCT-3´	5´-CGTCATCCATGGCGAACT-3´

IL, interleukin; TNF-α, tumor necrosis factor-α; NF-κB, nuclear factor kappa-light-chain-enhancer of activated B cells; OPG, osteoprotegerin; IFN-γ, interferon-γ; MMP-14, Matrix metalloproteinase-14; GAPDH, glyceraldehyde-3-phosphate dehydrogenase

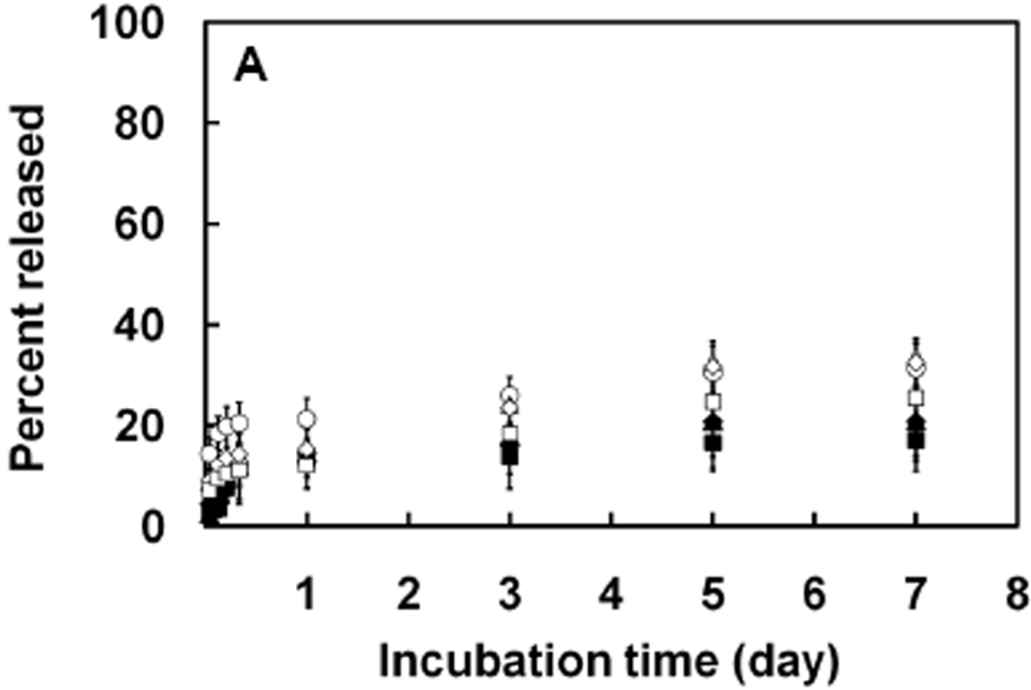

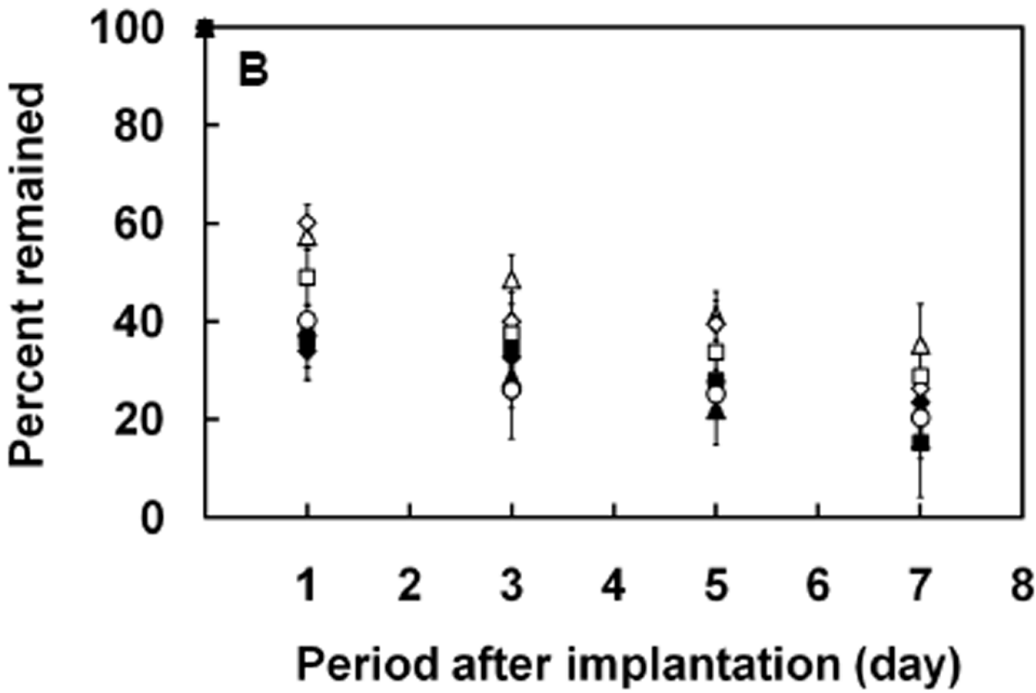

Figure 1 (Ratanavaraporn *et al.*)

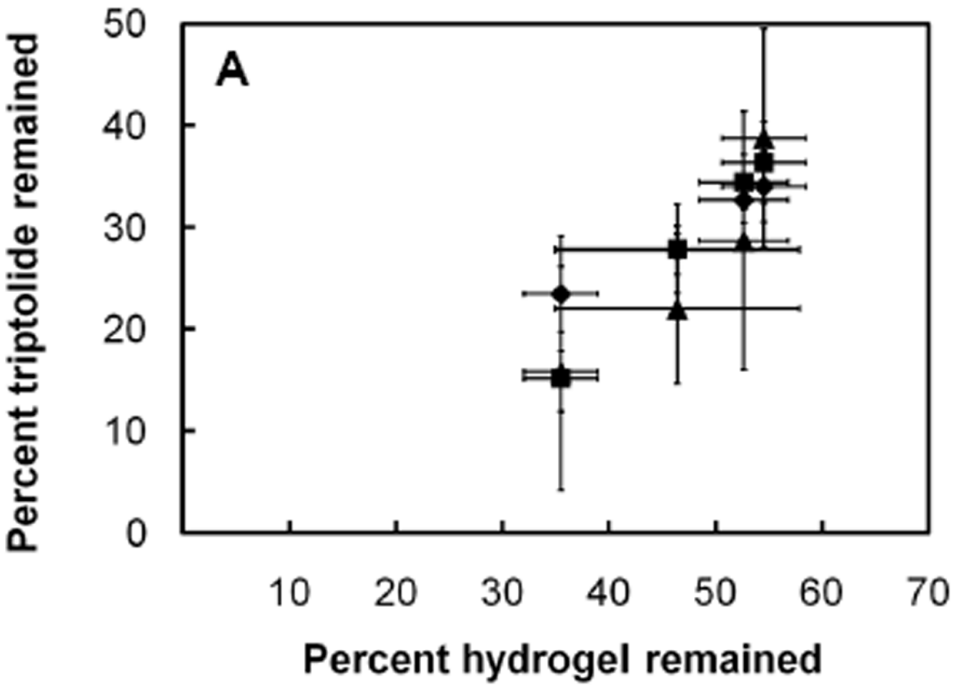

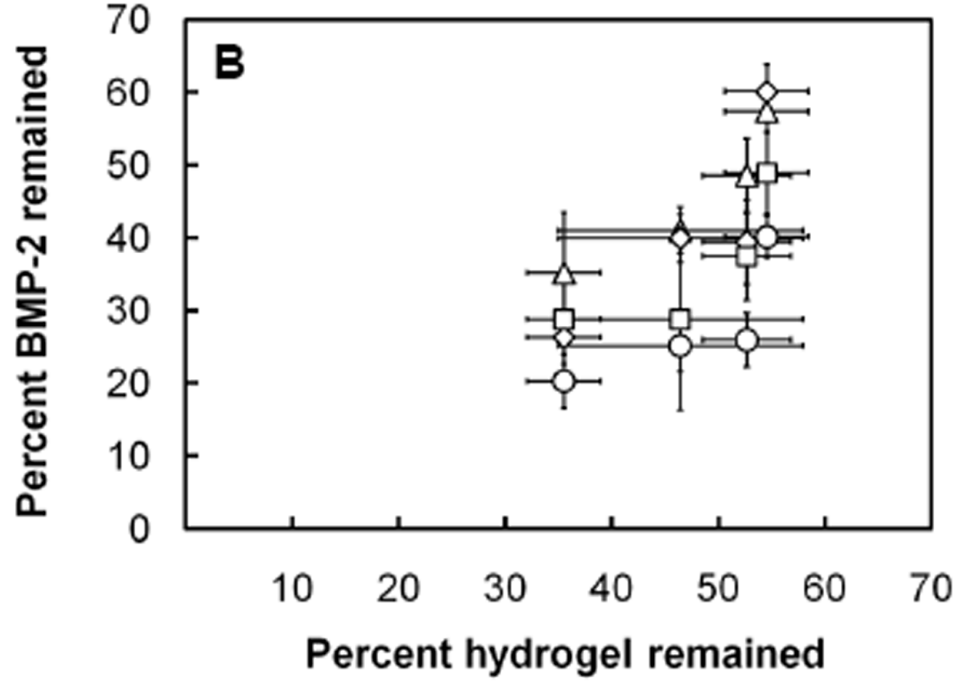

Figure 2 (Ratanavaraporn *et al.*)

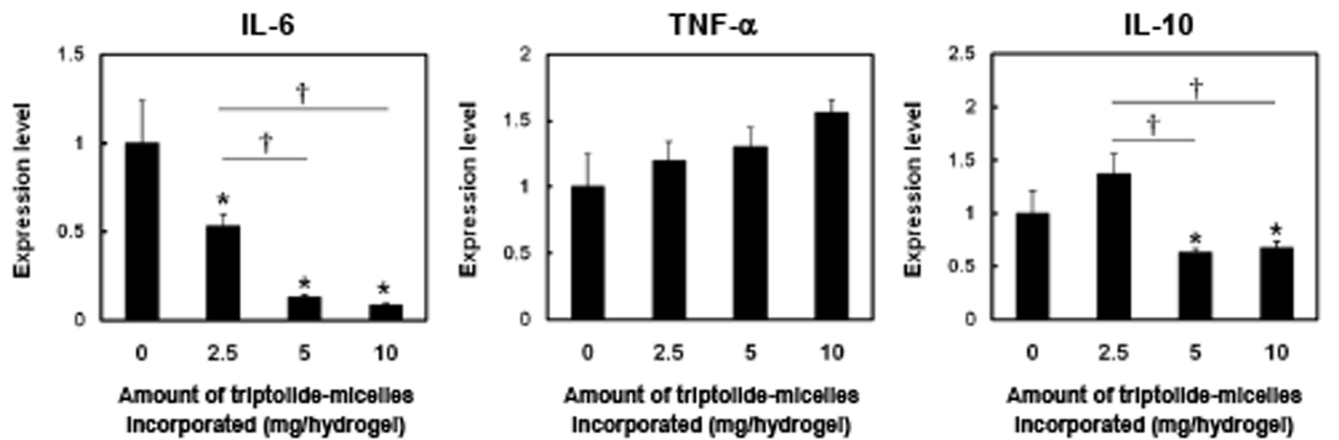

Figure 3 (Ratanavaraporn *et al.*)

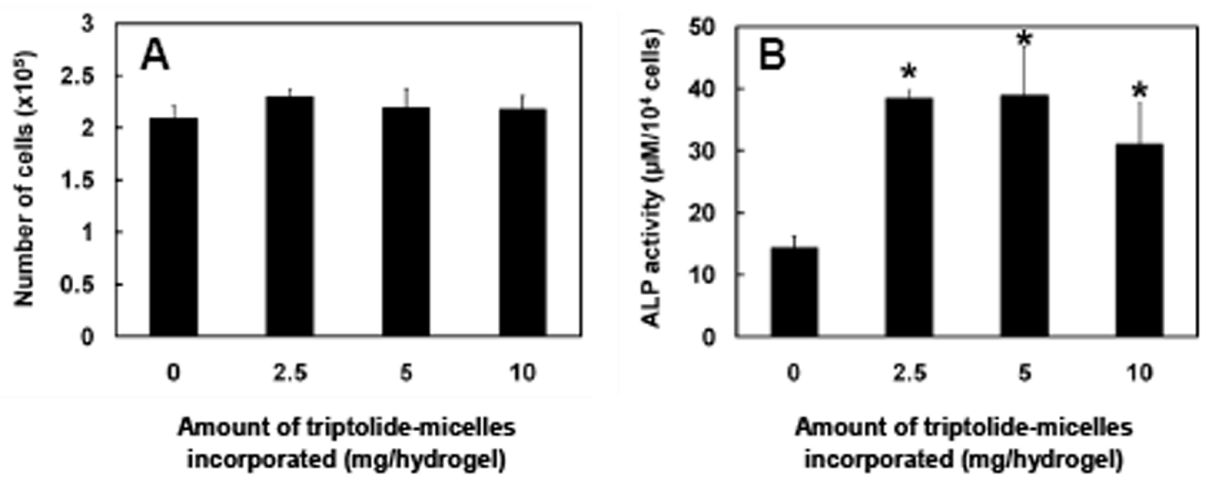

Figure 4 (Ratanavaraporn *et al.*)

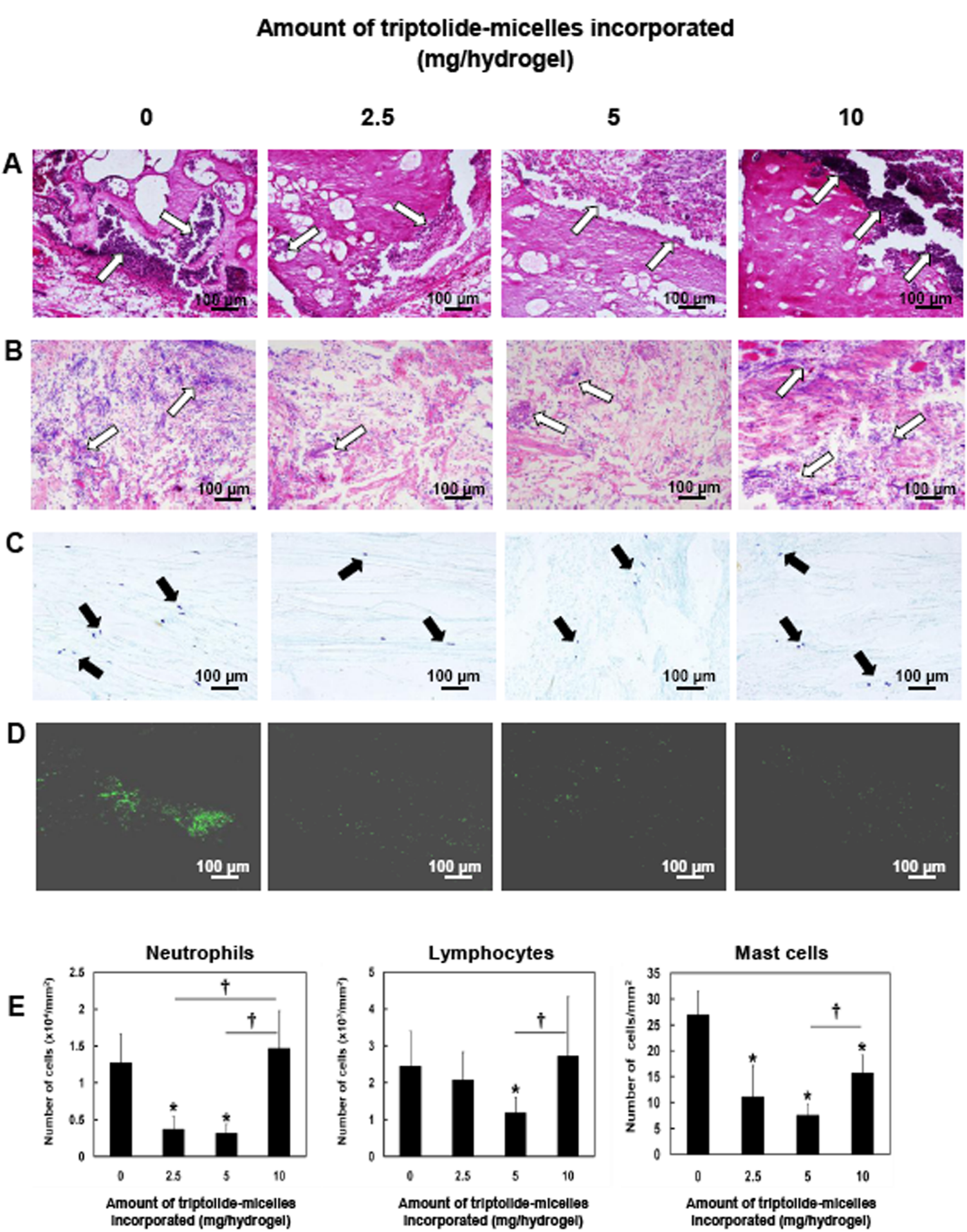

Figure 5 (Ratanavaraporn *et al.*)

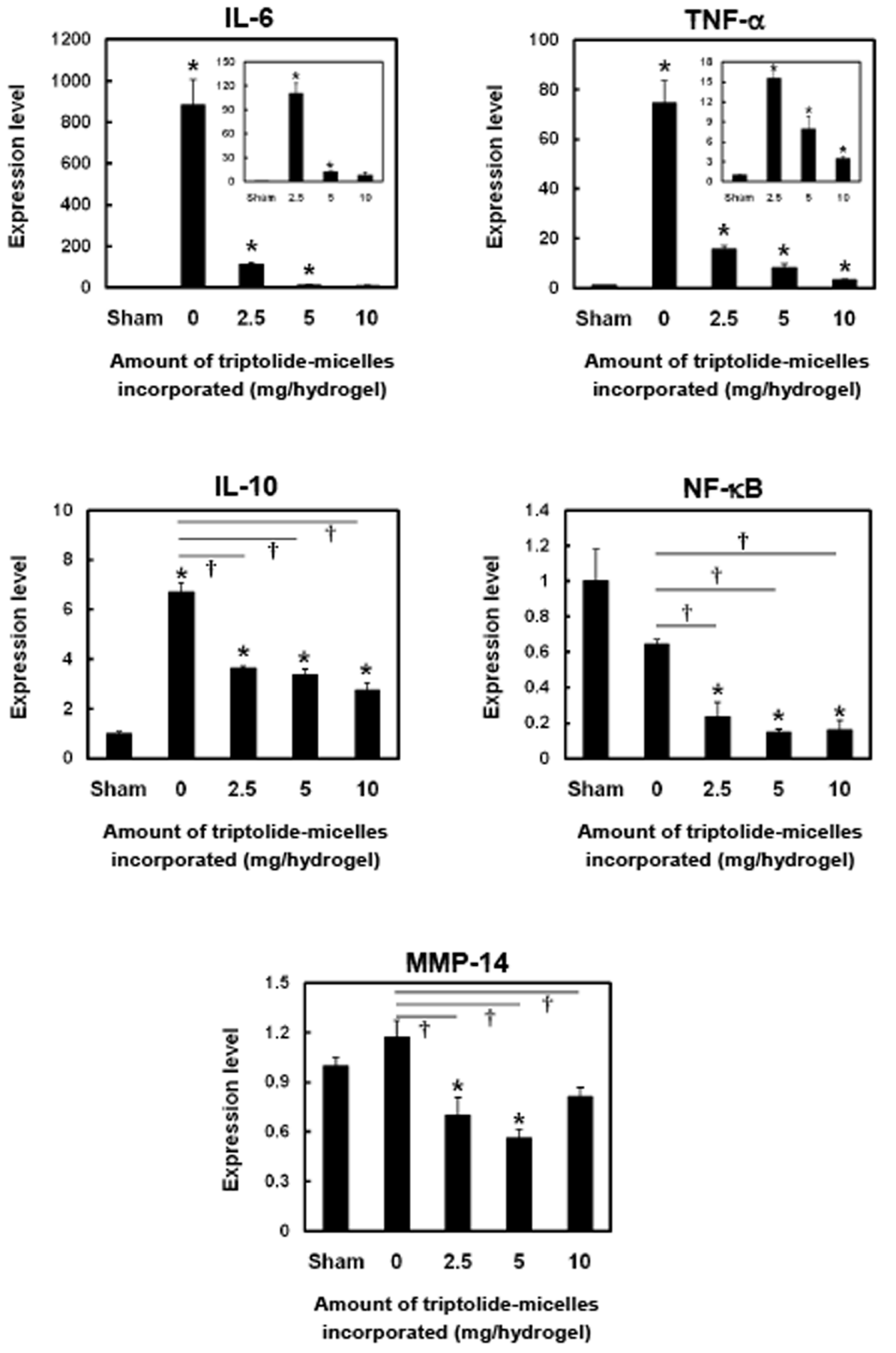

Figure 6 (Ratanavaraporn *et al.*)

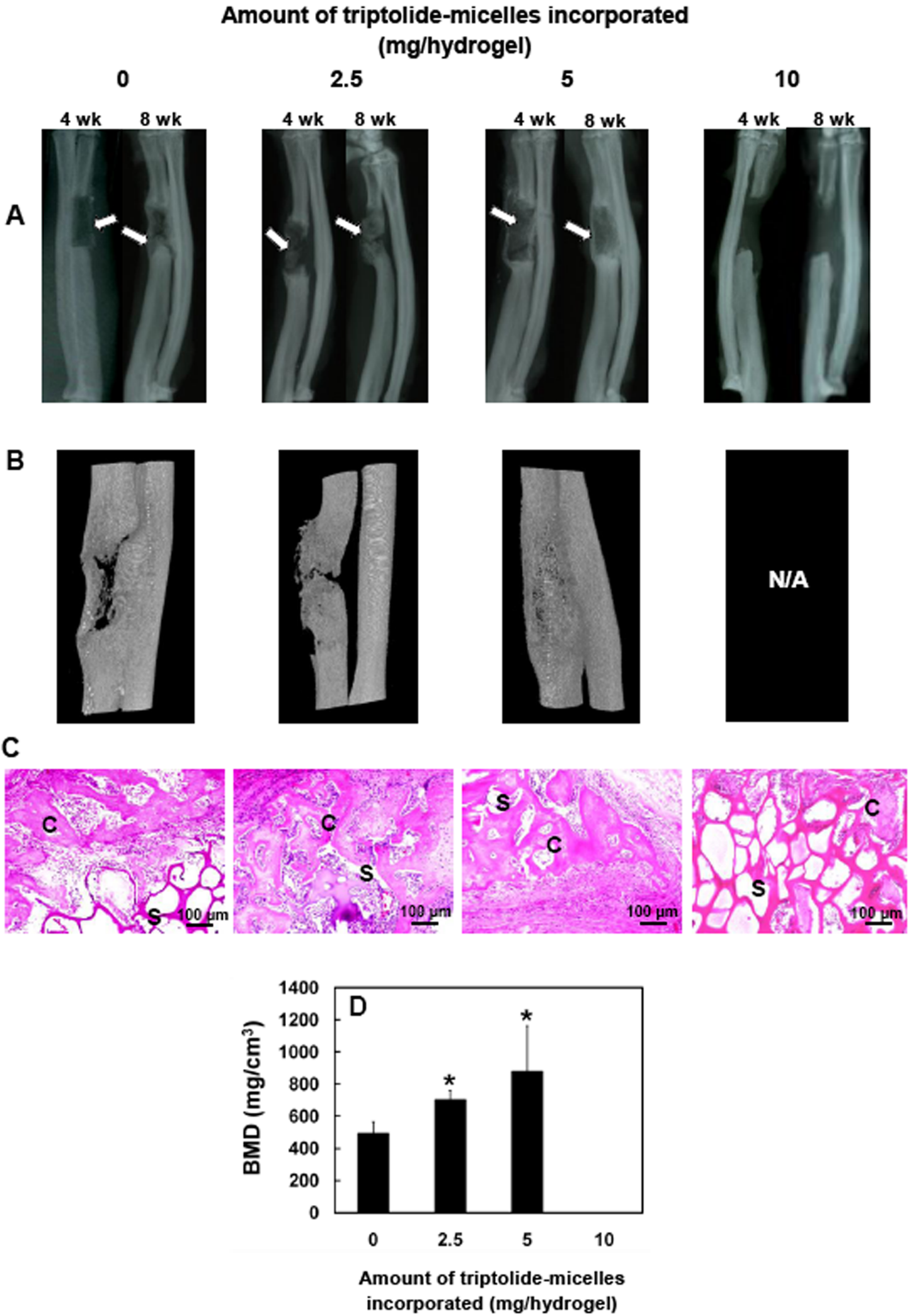

Figure 7 (Ratanavaraporn *et al.*)

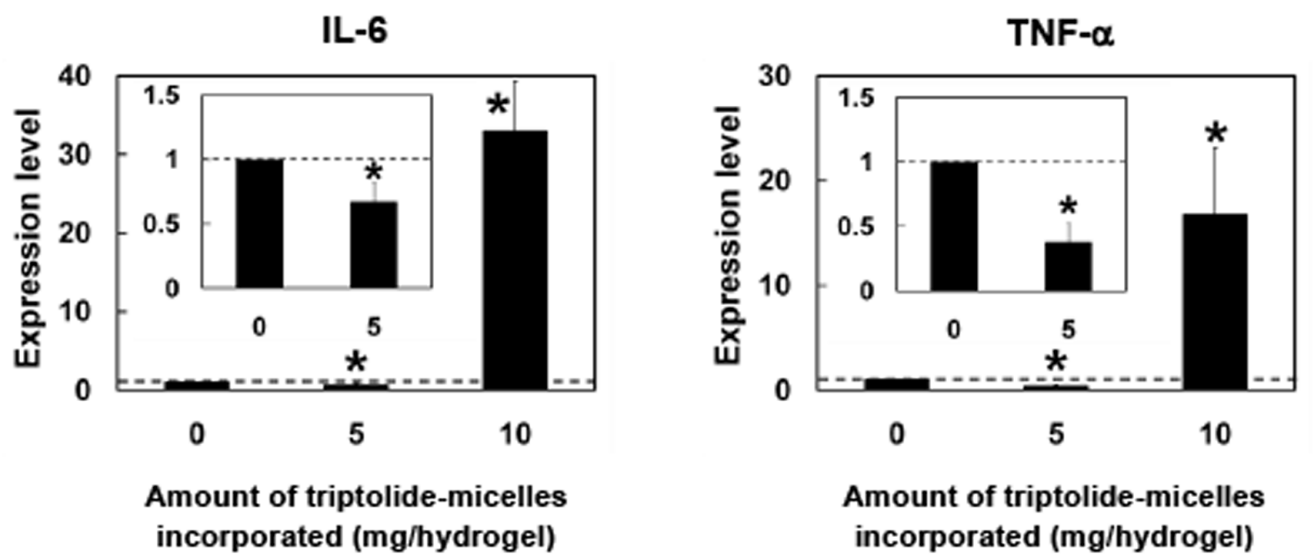

Figure S1 (Ratanavaraporn *et al.*)

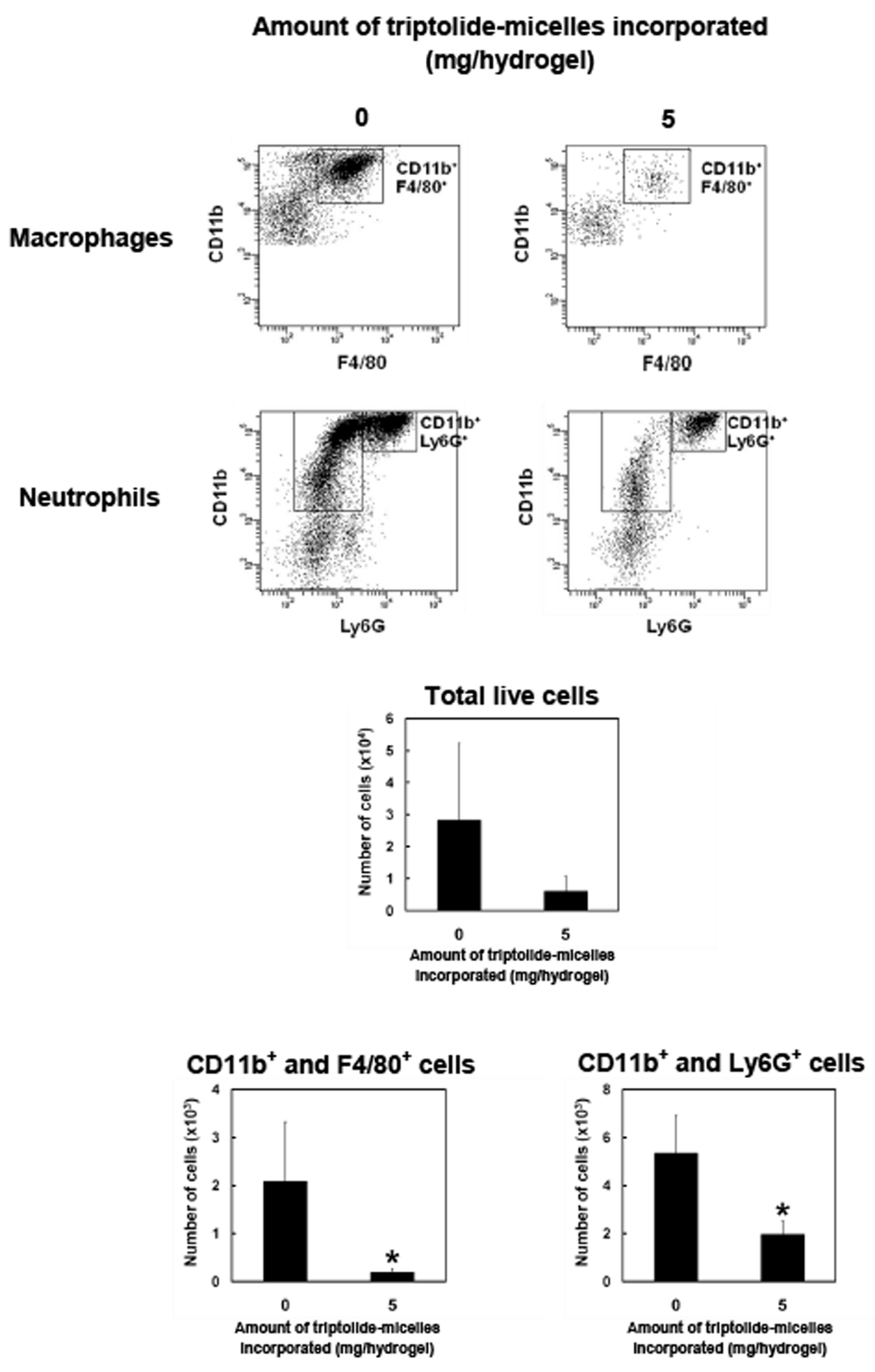

Figure S2 (Ratanavaraporn *et al.*)